

Raman spectra and dielectric properties of the nanocrystalline $\text{Li}_{0.43}\text{Nb}_{0.57}\text{O}_{3+\delta}$

Chia-Liang Kuo^a, Guo-Ju Chen^b, Chi-Shiung Hsi^c, Jian-Wen Wang^d, Yee-Shin Chang^e,
You-Yun Li^a, Weng-Sing Hwang^{a,*}

^aDepartment of Materials Science and Engineering, National Cheng Kung University, 1 Ta-Hsueh Road, Tainan 70101, Taiwan

^bDepartment of Materials Science and Engineering, I-Shou University, Kaohsiung, No.1, Section 1, Syuecheng Rd., Dasha District, Kaohsiung 84001, Taiwan

^cDepartment of Materials Science and Engineering, National United University, 1, Lienda, Miaoli 36003, Taiwan

^dDepartment of Environmental and Safety Engineering, Chung Hwa University of Medical Technology, 89 Wen-Hua 1st St., Jen-Te Hsiang, Tainan 71703, Taiwan

^eDepartment of Electronic Engineering, National Formosa University, 64 Wenhua Road, Huwei, Yunlin 632, Taiwan

Received 30 November 2012; received in revised form 13 August 2013; accepted 1 September 2013

Available online 7 September 2013

Abstract

The $\text{Li}_{0.43}\text{Nb}_{0.57}\text{O}_{3+\delta}$ material was synthesized by a combustion method and sintered at various temperatures. The crystal structure, surface morphology, and dielectric properties of the as-prepared lithium niobate bulks were characterized by X-ray diffraction (XRD), scanning electron microscopy (SEM), Raman spectrum and an LCR meter. After sintering at 1100 °C, the structure of the $\text{Li}_{0.43}\text{Nb}_{0.57}\text{O}_{3+\delta}$ was similar to the single crystal of lithium niobate. The thermal vibration of the elements caused the bond length of the Nb–O framework and angle bending of the O–Nb–O increase, and the structure was restored by the formation of square crystals in the quasi-melting $\text{Li}_{0.43}\text{Nb}_{0.57}\text{O}_{3+\delta}$ matrix. The dielectric constant increased with the increasing sintering temperature before 1000 °C, and then fell due the formation of a split seam. The reduction in defects forming from the Li-site vacancies lowered the dissipation factor at higher sintering temperatures.

© 2013 Elsevier Ltd and Techna Group S.r.l. All rights reserved.

Keywords: Lithium niobate; Dielectric constant; Phase split; Raman spectrum

1. Introduction

Materials with a perovskite structure, like BaTiO_3 , have some useful dielectric properties, such as high dielectric constant and low dielectric loss. The perovskite structure of niobium compounds, such as the NaNbO_3 , KNbO_3 , and LiNbO_3 , exhibits good dielectric and ferroelectric properties. Moreover, while lithium niobate and related materials have attracted wide research interest due to the promising optical properties of their single crystals, little work has been carried out to examine the dielectric and ferroelectric properties of lithium niobate, and most of the published studies focus on thin films rather than bulk materials. Examining the glass–ceramic produced by mixing lithium niobate powders with silica is the simplest way to study the dielectric properties of

this material, and the dielectric constant is function of the crystallization of the glass–ceramic of LiNbO_3 and SiO_2 [1–3]. In our previous study, the solubility of the lithium ions in the lithium niobate decreased with the increasing heat treatment temperature, and the lithium-rich secondary phase Li_3NbO_4 was observed in the stoichiometric lithium niobate [4]. In addition, the $\text{Li}_{0.43}\text{Nb}_{0.57}\text{O}_{3+\delta}$ material exhibited the pure phase of lithium niobate after being calcined at various temperatures.

In the current study, $\text{Li}_{0.43}\text{Nb}_{0.57}\text{O}_{3+\delta}$ material with the desired composition was synthesized by a combustion method. After being sintered at various temperatures, the crystal structure, dielectric properties, surface morphologies, and Raman spectra were observed, and these are reported in detail below.

2. Experimental procedures

In our previous studies, nano-scaled lithium niobate powders were synthesized by a combustion method and the phase

*Corresponding author. Tel.: +886 6 2757575x62928;

fax: +886 6 2344393.

E-mail address: wshwang@mail.ncku.edu.tw (W.-S. Hwang).

transformations that occurred at high temperatures were also reported [4,5]. In this work, the structural transformation was examined, along with the dielectric properties of the $\text{Li}_{0.43}\text{Nb}_{0.57}\text{O}_{3+\delta}$ at various temperatures. The starting materials of lanthanum nitrate, ammonium niobate oxalate hydrate, and glycine had a purity of at least 99.4%. The stoichiometric solution was bathed at 80 °C, so that it was viscous, and then calcined at 600 °C for 1 h. Finally, the calcined powders were pressed into disks at 200 MPa with a diameter of 10–11 mm and thickness of 2–3 mm. The disks were sintered at various temperatures for 2 h at the heating rate of 3 °C/min, and then cooled to room temperature at the same rate. The crystal structures were examined by the analyses of X-ray diffraction and Raman spectroscopy. The X-ray patterns were performed on a Rigaku diffractometer (RAD-II A) using monochromatized CuK α radiation ($\lambda=0.15406$ nm). The Raman spectra were recorded on a Horiba Jobin Yvon HR Raman spectrometer. A typical 785 nm wavelength diode laser was used to excite the samples and scans were taken on an extended range 100–1000 cm^{-1} . The microstructures were investigated using a Hitachi Field Emission Scanning Electron Microscope (S4700). The dielectric properties were measured between In–Ga electrodes applied to the top and bottom of the ground disk. The measurements of the dielectric properties were made at the frequency of 1000 KHz using an LCR meter (HP4284A).

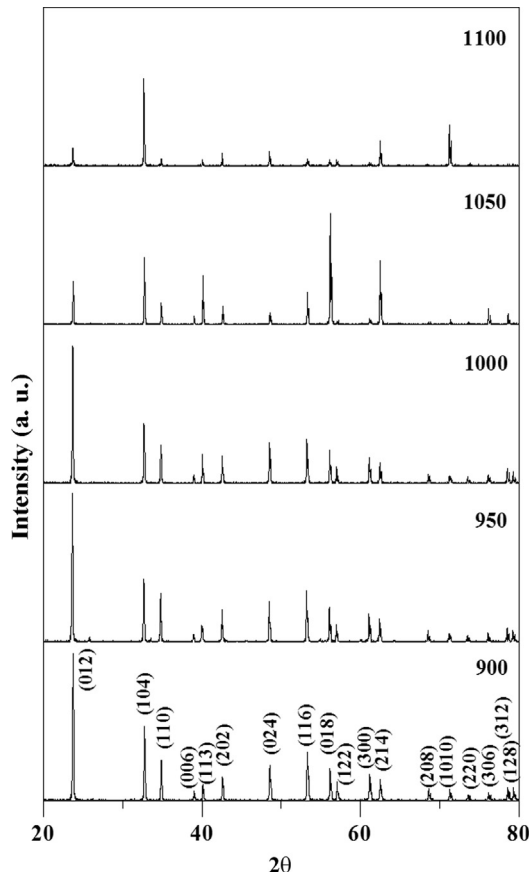


Fig. 1. X-ray diffraction patterns of $\text{Li}_{0.43}\text{Nb}_{0.57}\text{O}_{3+\delta}$ sintered at various temperatures for 2 h.

3. Results and discussion

Fig. 1 shows the structural transformation of the $\text{Li}_{0.43}\text{Nb}_{0.57}\text{O}_{3+\delta}$ powders sintered at various temperatures for 2 h. The XRD results indicate that some planes had abnormal growth with the increasing sintering temperature. The intensity of peaks like (012), (110), (024) and (300) decreased with increase of the sintering temperature. The peaks of (113), (018) and (214) planes became strong as the calcination temperature increased, but diminished when the temperature was close to the melting point.

It is inferred that the grain growth followed the crystal habits with the increasing calcination temperature, the elements rearranged with the loosening bonding energy and migrated to the planes with the lower free energy, which resulted that intensities of peaks (012), (110), (024) and (300) decreased and transition planes of the quasi-sintered lithium niobate like (113), (018) and (214) became intense. When the sintering temperature (1100 °C) was near the melting point (1130 °C), the nano-particles of lithium niobate started to melt, the elements tended to rearrange in the *c*-axis, and the transition planes diminished. The structure of lithium niobate bulk became similar to that of a single crystal, the number of crystalline planes decreased obviously, and the three strongest peaks were (104), (214), and (1010).

The Raman spectra of polycrystalline lithium niobate sintered at various temperature are given in Fig. 2. It can be seen that with the increasing sintering temperature, the relative strength of the peak appearing at 239 cm^{-1} compared to the others was weakening before sintered at 1050 °C, and then recovered after 1100 °C. The peak position at 239 cm^{-1} may be associated with the deformation of the Nb–O framework, and the potential energy distribution (PED) with the frequency of 255 cm^{-1} was contributed by the O–Nb–O angle bending [6]. The frequencies of 251 and 258 cm^{-1} can be considered as the red and blue shifts of 255 cm^{-1} . When the

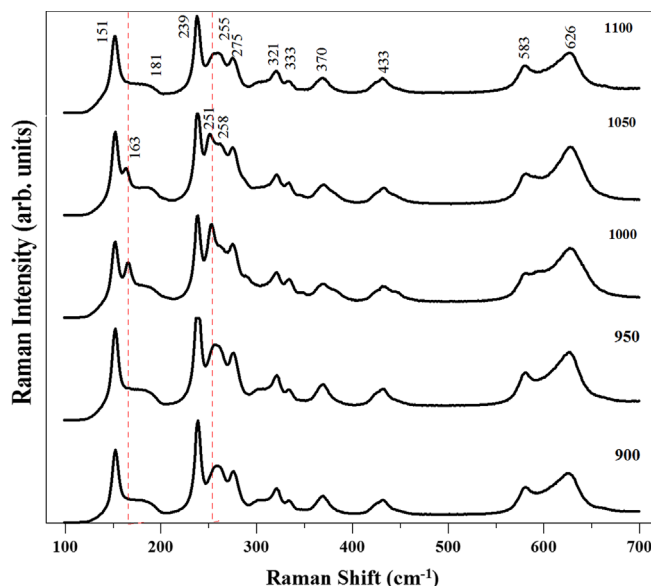


Fig. 2. Raman spectra of polycrystalline $\text{Li}_{0.43}\text{Nb}_{0.57}\text{O}_{3+\delta}$ sintered at various temperatures for 2 h.

lithium niobate was sintered, the longer distance and greater angle of the Nb–O framework made it easy for the bonds to break, causing the structure of the $\text{Li}_{0.43}\text{Nb}_{0.57}\text{O}_{3+\delta}$ crystal to split. The subsequent lithium deficiency left vacancy sites in the $\text{Li}_{0.43}\text{Nb}_{0.57}\text{O}_{3+\delta}$ crystal, and the $\text{Li}_{0.91}\text{NbO}_3$ and LiNbO_3 structure formed to reduce the lattice distortion in the sintering process [5]. The coexistence of these two phases lead to both tensile and compressive stress in the lithium niobate, with the O–Nb–O angle bending increasing and reducing, respectively. As the sintering temperature reached the highest point, the angle bending of O–Nb–O was restored to its original state. The frequency of 163 cm^{-1} has not been observed before in the literature, and its appearance may due to the intermediate phase transition.

The dielectric properties of $\text{Li}_{0.43}\text{Nb}_{0.57}\text{O}_{3+\delta}$ bulk sintered at various temperatures are shown in Fig. 3. After being sintered

at 900°C , the dielectric constant was in the range of 500–800, and a great amount of diffuse phase transition (DPT) was observed due to the nonstoichiometric lithium niobate defects. As the sintering temperature increased, the DPT effect decreased due to the reduction in lattice distortion by phase splitting. The dielectric constant rose along with the sintering temperature until 950°C , fell slightly at 1000°C , and then dropped as the structure changed at higher sintering temperatures. The dielectric properties of lithium niobate depend on the mobility of the lithium ions [7]. According to the Raman spectra, the frequency of 151 cm^{-1} did not shift when sintered at various temperatures, and the concentration of lithium in the lithium niobate remained the same. In the $\text{Li}_{0.43}\text{Nb}_{0.57}\text{O}_{3+\delta}$ material some of the Nb ions occupied the Li-site vacancies to form an intrinsic *n*-type semiconductor. While sintering, the oxygen diffused from the grain boundary into the conductive oxygen-deficient structure, and the $\text{Li}_{0.43}\text{Nb}_{0.57}\text{O}_{3+\delta}$ material can be considered a grain boundary barrier layer (GBBL) capacitor. The fall in the dielectric constant was due to the reduction in the grain boundary and formation of cracks when cooling from relative high temperatures. The defects of the Li-site vacancies of the nonstoichiometric lithium niobate reduced during phase splitting in the subsequent sintering process. The number of defects and amount of porosity were both reduced, leading to the lower dissipation factor.

The diameter of the as-prepared $\text{Li}_{0.43}\text{Nb}_{0.57}\text{O}_{3+\delta}$ powders was in the range of 29–38 nm [4,5]. The size of the powders increased rapidly when the heat treatment was close to the melting temperature. Fig. 4(e) shows some square crystals and a split seam in the melting lithium niobate matrix, and these seem to grow during the cooling process. The usual way to produce single crystals of lithium niobate is to use the seeding method with the melting solution [8]. However, in this work no lithium niobate seed was used, and the quasi-liquid lithium niobate still formed small square crystals with a slow cooling rate. The XRD results show that the diffraction peaks of the sintered bulk are similar to those of the single crystal structure. The three strongest diffraction planes, (104), (214), and (1010), perhaps correspond to the square crystals, and the other indistinct peaks belong to the matrix structure.

4. Conclusions

The polycrystalline $\text{Li}_{0.43}\text{Nb}_{0.57}\text{O}_{3+\delta}$ material exhibits the pure phase of lithium niobate after being sintered at various temperatures. As the sintering temperature rises to near the melting temperature, the $\text{Li}_{0.43}\text{Nb}_{0.57}\text{O}_{3+\delta}$ matrix becomes quasi-liquid, and then crystallizes in the slow cooling process. After sintering at 1100°C , square crystals are observed in the SEM image, and perhaps correspond to the three strongest diffraction peaks of (104), (214), and (1010). The dielectric constant of the polycrystalline $\text{Li}_{0.43}\text{Nb}_{0.57}\text{O}_{3+\delta}$ material increases before 1000°C , and decreases with the formation of cracks and reduction in grain boundary. In addition, the dissipation factor decreases for the denser structure and lower defect concentration of the material after sintering at higher temperatures.

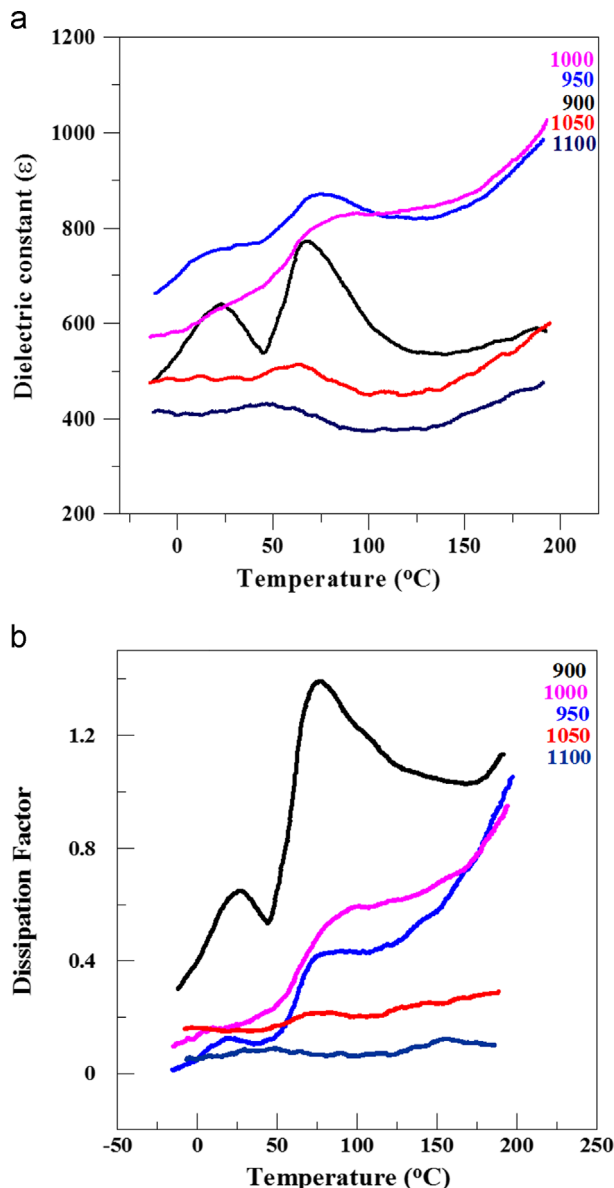


Fig. 3. (a) Dielectric constant and (b) dissipation factor at temperatures 1 KHz for $\text{Li}_{0.43}\text{Nb}_{0.57}\text{O}_{3+\delta}$ sintered at various temperatures for 2 h.

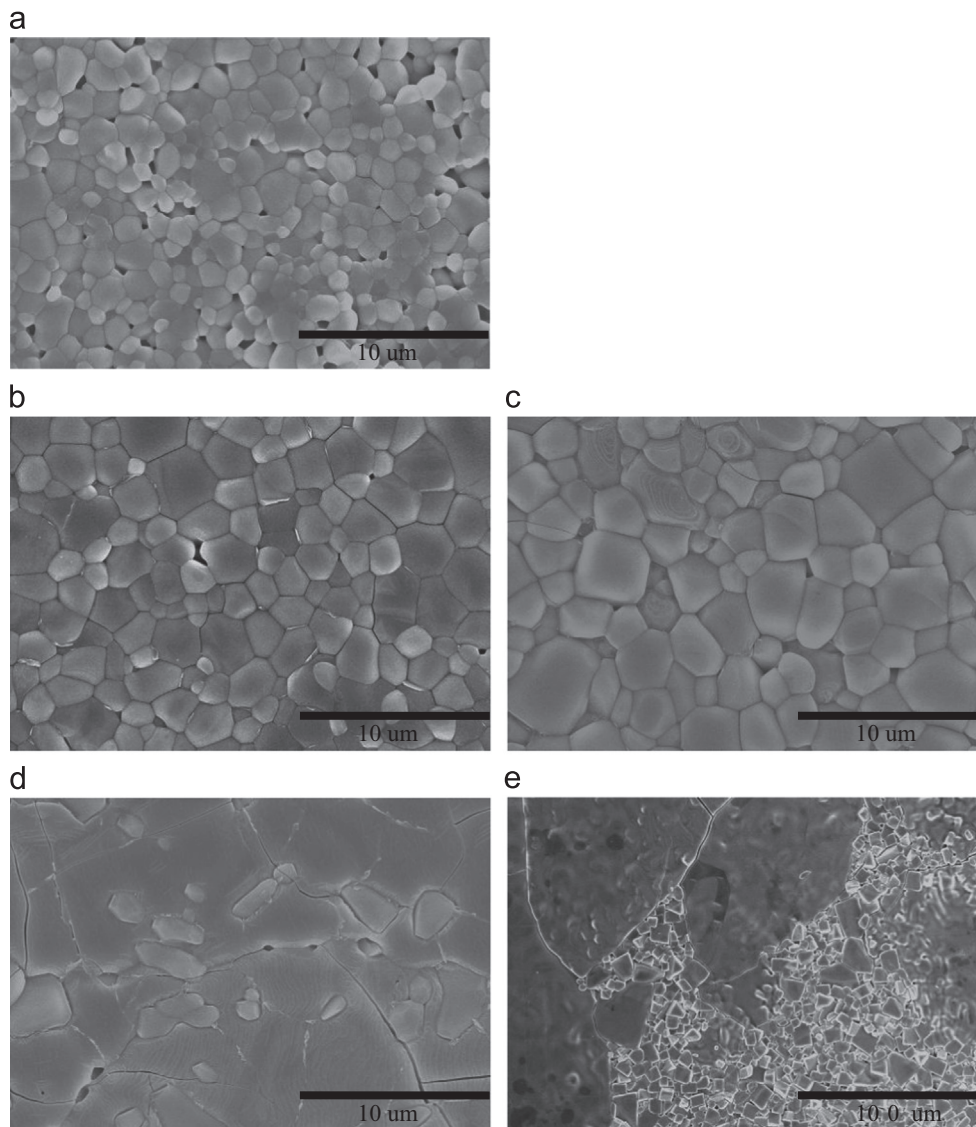


Fig. 4. SEM images of $\text{Li}_{0.43}\text{Nb}_{0.57}\text{O}_{3+\delta}$ sintered at various temperatures for 2 h. (a) 900 °C, (b) 950 °C, (c) 1000 °C, (d) 1050 °C, and (e) 1100 °C.

Acknowledgments

A part of the present work was also supported by the Research Center for Energy Technology and Strategy (D102-23002), at National Cheng Kung University in Taiwan.

References

- [1] M.P.F. Graca, M.G. Ferreira da Silva, M.A. Valente, Dielectric and structural studies of a $\text{SiO}_2\text{--Li}_2\text{O--Nb}_2\text{O}_5$ glass and glass-ceramic prepared by the sol–gel method, *Journal of Non-Crystalline Solids* 351 (2005) 2951–2957.
- [2] J.E. Kim, S.J. Kim, Ken-ichi Ohshima, Y.H. Hwang, Y.S. Yang, Crystallization and dielectric properties of $4\text{LiNbO}_3\text{--SiO}_2$ glass, *Materials Science and Engineering A: Structural Materials: Properties, Microstructure and Processing* 375–377 (2004) 1255–1258.
- [3] P. Prapitpongwanich, R. Harizanova, K. Pengpat, C. Rüssel, Nanocrystallization of ferroelectric lithium niobate in $\text{LiNbO}_3\text{--SiO}_2$ glasses, *Materials Letters* 63 (2009) 1027–1029.
- [4] C.L. Kuo, Y.S. Chang, Y.H. Chang, W.S. Hwang, Synthesis of nanocrystalline lithium niobate powders via a fast chemical route, *Ceramics International* 37 (2011) 951–955.
- [5] C.L. Kuo, G.J. Chen, Y.S. Chang, J.X. Fu, Y.H. Chang, W.S. Hwang, Thermal behavior of the nonstoichiometric lithium niobate powders synthesized via a combustion method, *Ceramics International* 38 (2012) 3729–3733.
- [6] Y. Repelon, E. Husson, F. Bennani, C. Proust, Raman spectroscopy of lithium niobate and lithium tantalate. Force field calculations, *Journal of Physics and Chemistry of Solids* 60 (1999) 819–825.
- [7] A.M. Glass, K. Nassau, T.J. Negran, Ionic conductivity of quenched alkali niobate and tantalate glasses, *Journal of Applied Physics* 49 (1978) 4808–4811.
- [8] I. Franke, E. Talik, K. Roleder, K. Polgár, J.P. Salvestrini, M.D. Fontana, Temperature stability of elastic and piezoelectric properties in LiNbO_3 single crystal, *Journal of Physics D: Applied Physics* 38 (2005) 4308–4312.